Available online at www.sciencedirect.com
ScienceDirect
International Journal of Multiphase Flow 33 (2007) 86–100
International Journal of Multiphase Flow
www.elsevier.com/locate/ijmulflow

Pressure calculations in disperse and continuous multiphase flows

Duan Z. Zhang *, W. Brian VanderHeyden [1], Qisu Zou, Nely T. Padial-Collins [2]

Theoretical Division, Fluid Dynamics Group T-3, B216 Los Alamos National Laboratory, Los Alamos, NM 87545, USA

Received 20 July 2006; received in revised form 27 July 2006

Abstract

In many models for disperse two-phase flows, the pressure of the disperse phase is often assumed to be the same as that of the continuous phase, or differ only by an amount caused by the surface tension. This type of model is referred to as an equilibrium pressure model. Recent research indicates that the stress difference between the phases caused by dynamics of the motion can be significantly important in the modeling of disperse two-phase flows. Although this difference is still ignored in most calculations of disperse multiphase flows for various reasons, when an equilibrium pressure model is applied to continuous multiphase flows, a conceptual difficulty arises. For instance, the equilibrium pressure model cannot be used to study the tensile break of a sponge with interconnected pores, because the air in the pores can never go into tension while the sponge material does not break without tension.

To avoid this conceptual difficulty, a multipressure model is introduced for continuous multiphase flows by analyzing and then modifying the implicit assumption about the volumetric strain rates involved in the equilibrium pressure model. Numerical implementations of the multipressure model are discussed. An example using the multipressure model is presented.

Published by Elsevier Ltd.

Keywords: Multipressure model; Continuous multiphase flows

1. Introduction

Considerable work has been devoted to the study of disperse multiphase flows, in which there is only one continuous phase and all other phases are in forms of particles, droplets and bubbles with sizes small compared to the macroscopic length scale of the flow. A continuous multiphase flow, in contrast, contains more than one continuous phase occupying regions or forming interconnected networks with length scales comparable to the macroscopic length scale of the flow. There are relatively few studies conducted on

* Corresponding author. Tel.: +1 505 665 4428; fax: +1 505 665 5926.
E-mail address: dzhang@lanl.gov (D.Z. Zhang).
[1] International and Applied Technology Division, International Research, Analysis and Technology Group.
[2] Computer and Computational Science Division, Continuum Dynamics Group.

0301-9322/$ - see front matter Published by Elsevier Ltd.
doi:10.1016/j.ijmultiphaseflow.2006.07.006

continuous multiphase flows as compared to the number of studies of disperse multiphase flows. Part of the reason for this is the difficulties related to the description of the morphology of continuous multiphase flows.

Advances in the materials manufacturing industry have produced many interesting composites with continuous or interpenetrating material phases (Wegner and Gibson, 2000; Feng et al., 2003). On the numerical front, advances of the particle-in-cell method (Harlow and Amsden, 1991; Sulsky and Brackbill, 1991; Cummins and Brackbill, 2002) enable the computational study of fluid–structure interactions using the method of multiphase flows (Ma et al., 2005). In this method the solid and fluid are treated as interpenetrating two-phase flows. The stresses in the solid and in the fluid are governed by different constitutive relations. All of these developments enable the study of continuous multiphase flow or the deformation of the interpenetrating composite materials.

One of the most important differences between the disperse and continuous multiphase flows resides in the character of phase interactions. It has been shown that the phase interactions go beyond the exchange forces (such as drag, added mass force etc). In addition to the surface tension effects, the difference in the average stresses between the phases results from the dynamics of phase interactions. This dynamical part of the stress difference has important consequences to a multiphase flow. The dynamical part of the pressure difference for potential flows was first studied by Stuhmiller (1977). Later, Zhang and Prosperetti (1994) found that phase interactions not only result in the pressure difference but also a stress in a potential flow. For low Reynolds number flows the dynamical stress difference is related to effective viscosity (Zhang and Prosperetti, 1997). Despite its importance (Hwang and Shen, 1989; Sangani and Didwania, 1993; Prosperetti, 1999), the dynamical part of the stress difference is largely ignored in calculations of disperse multiphase flows. Part of the reason for ignoring this important part of the stress difference is related to the uncertainties (Sundaresan, 2000) in the models for disperse multiphase flows. The other part of the reason is that it does not result in obvious conceptual difficulties in disperse multiphase flows. Models with the dynamical part of the stress or pressure difference ignored are referred to as equilibrium pressure models. In continuous multiphase flows, the dynamical part of the stress difference can no longer be ignored. The example of a sponge made of elastic material in tension with fluid-filled pores illustrates the critical nature of the stress difference.

In this paper, instead of examining the full tensorial stress difference, we focus only on the pressure difference, or isotropic component of the stress difference. The first reason for this choice is that the pressure is directly related to the volumetric strain of the material and that the continuity condition provides a constraint to the rates of volumetric deformations. We examine the consequence of this constraint in this paper. The second reason is that, in many flows, such as the Rayleigh–Taylor mixing problem (Ramshaw, 1998), the motion is dominated by the inertia and pressure; and the deviatoric component of the stress can be neglected. The third reason is, that the study of the isotropic component of the stress may provide guidance in the study of the deviatoric components.

The pressure in a compressible material depends on the volumetric deformation. In many numerical calculations of multiphase flows the average phase pressure is not determined directly by calculating the volumetric deformation of the material, rather it is determined by requiring that all volume fractions sum to one (Prosperetti and Tryggvason, 2006). Therefore the numerical scheme implies a method of calculating the volumetric deformations of the phases. In this paper, we study the assumptions involved in the method and then modify them to reach a multipressure model while still satisfying the continuity requirement.

As an example, this multipressure model is then used in Section 6, to calculate the spalling of a porous solid with interconnected pores in the presence of the air – a continuous two-phase problem. The pressure field for the air and the stress field for the solid are calculated at the same time. This example shows that the multipressure model introduced can be used to study fluid–structure interaction problems in the context of continuous multiphase flows.

2. Averaged equations for multimaterial flows

Averaged equations for multiphase flows can be derived using a number of approaches. In this paper, we extend the ensemble average approach used by Zhang and Prosperetti (1994), Zhang and Prosperetti (1997). In their approach the probability is defined in a phase space comprised of the coordinates and velocities of the particle centers. In the study of continuous multiphase flows, such as turbulent mixing problems, the number

of the degrees of freedom in the flow is not finite. The concept of the probability defined on the finite dimensional phase space needs to be extended slightly. Such an extension (Drew and Passman, 1999) requires some mathematical formality and a few concepts of real analysis. So that we are not burdened by mathematics, we explain the ensemble average, the associated probability and the relation of the probability to the probability density used by Zhang and Prosperetti (1994), Zhang and Prosperetti (1997) in Appendix A. The main conclusion from Appendix A is that the forms of the averaged equations derived by Zhang and Prosperetti for systems with finite degrees of freedom are also correct for systems with an infinite number of degrees of freedom, and therefore are applicable to disperse multiphase flows with finite Reynolds number. For continuous multiphase flows, however, the small particle approximation previously used is not applicable and needs to abandoned. We study the consequence of this abandonment.

We consider an ensemble of flows and denote a flow belonging to the ensemble as $\mathscr{F}$. Let $C_i(\boldsymbol{x}, t, \mathscr{F})$ be the indicator function of phase i, such that $C_i(\boldsymbol{x}, t, \mathscr{F}) = 1$ if the spatial point $\boldsymbol{x}$ is occupied by phase i in flow $\mathscr{F}$ at time t, and $C_i(\boldsymbol{x}, t, \mathscr{F}) = 0$, otherwise. The volume fraction θ_i of phase i at this point at time t is calculated by averaging the values of the indicator functions over all possible flows in the ensemble.

$$\theta_i(\boldsymbol{x}, t) = \int C_i(\boldsymbol{x}, t, \mathscr{F}) \mathrm{d}\mathscr{P}, \tag{1}$$

where $\int(\cdot)\mathrm{d}\mathscr{P}$ denotes the average over all possible flows in the ensemble.

The gradient of the volume fraction is calculated as

$$\nabla\theta_i = \int \nabla C_i(\boldsymbol{x}, t, \mathscr{F}) \mathrm{d}\mathscr{P}. \tag{2}$$

The ensemble phase average $\langle q_i \rangle$ for a quantity q_i pertaining to phase i is defined as

$$\theta_i \langle q_i \rangle(\boldsymbol{x}, t) = \int C_i(\boldsymbol{x}, t, \mathscr{F}) q_i(\boldsymbol{x}, t, \mathscr{F}) \mathrm{d}\mathscr{P}, \tag{3}$$

and its gradient is calculated as

$$\theta_i \nabla \langle q_i \rangle(\boldsymbol{x}, t) = \theta_i \langle \nabla q_i \rangle(\boldsymbol{x}, t) + \int [q_i(\boldsymbol{x}, t, \mathscr{F}) - \langle q_i \rangle(\boldsymbol{x}, t)] \nabla C_i(\boldsymbol{x}, t, \mathscr{F}) \mathrm{d}\mathscr{P}, \tag{4}$$

after using (2).

For a velocity field $\boldsymbol{u}_i(\boldsymbol{x}, t)$ of phase i, by replacing q_i with $\boldsymbol{u}_i q_i$ in (3), differentiating the equation with respect to $\boldsymbol{x}$ and then adding the resulting equation to the partial time derivative of (3), we find the averaged transport equation for the quantity q_i

$$\frac{\partial}{\partial t}(\theta_i \langle q_i \rangle) + \nabla \cdot (\theta_i \langle \boldsymbol{u}_i q_i \rangle) = \theta_i \left\langle \frac{\partial q_i}{\partial t} + \nabla \cdot (\boldsymbol{u}_i q_i) \right\rangle + \int \dot{C}_i q_i \mathrm{d}\mathscr{P}, \tag{5}$$

after exchanging the time and spatial differentiation with the probability integral, where

$$\dot{C}_i = \frac{\partial C_i}{\partial t} + \boldsymbol{u}_i \cdot \nabla C_i. \tag{6}$$

The last term in (5) represents a source or a sink to quantity q_i due to phase change in the flows in the ensemble.

The averaged mass conservation equation can be obtained from the averaged transport Eq. (5) by setting $q_i = \rho_i^0$, where ρ_i^0 is the material density, or the microscopic density, of phase i.

$$\frac{\partial}{\partial t}(\theta_i \langle \rho_i^0 \rangle) + \nabla \cdot (\theta_i \tilde{\boldsymbol{u}}_i \langle \rho_i^0 \rangle) = \int \rho_i^0 \dot{C}_i \mathrm{d}\mathscr{P}, \tag{7}$$

where $\tilde{\boldsymbol{u}}_i$ is the Favre averaged velocity defined as $\tilde{\boldsymbol{u}}_i \langle \rho_i^0 \rangle = \langle \boldsymbol{u}_i \rho_i^0 \rangle$.

By setting $q_i = 1$ in (5) one finds the evolution equation for the volume fraction

$$\frac{\partial \theta_i}{\partial t} + \nabla \cdot (\theta_i \langle \boldsymbol{u}_i \rangle) = \theta_i \langle \nabla \cdot \boldsymbol{u}_i \rangle + \int \dot{C}_i \mathrm{d}\mathscr{P}. \tag{8}$$

Adding $\nabla \cdot [\theta_i(\tilde{\boldsymbol{u}}_i - \langle \boldsymbol{u}_i \rangle)]$ to both sides of (8), using (2) and the definition (3) of an averaged quantity we have

$$\frac{\partial \theta_i}{\partial t} + \tilde{\boldsymbol{u}}_i \cdot \nabla \theta_i = \int \dot{C}_i \mathrm{d}\mathscr{P} - \int (\boldsymbol{u}_i - \tilde{\boldsymbol{u}}_i) \cdot \nabla C_i \mathrm{d}\mathscr{P}. \tag{9}$$

Multiplying (9) by $\langle \rho_i^0 \rangle$ and then subtracting the resulting equation from (7) we have the averaged evolution equation for the average of the microscopic density.

$$\theta_i \left[\frac{\partial \langle \rho_i^0 \rangle}{\partial t} + \nabla \cdot (\tilde{\boldsymbol{u}}_i \langle \rho_i^0 \rangle) \right] = \int (\rho_i^0 - \langle \rho_i^0 \rangle) \dot{C}_i \mathrm{d}\mathscr{P} + \langle \rho_i^0 \rangle \int (\boldsymbol{u}_i - \tilde{\boldsymbol{u}}_i) \cdot \nabla C_i \mathrm{d}\mathscr{P}. \tag{10}$$

While the right hand sides of (9) and (10) can be written in mathematically simpler forms by using (6), in this paper we choose to leave them in the forms presented above because in many cases, models for phase changes are given for $\dot{Z}_i$. Our task in this paper is to study constraints on the closures for the interface integral $\int (\boldsymbol{u}_i - \tilde{\boldsymbol{u}}_i) \cdot \nabla C_i \mathrm{d}\mathscr{P}$.

The multiphase flow momentum equation can be derived by setting $q_i = \rho_i^0 \boldsymbol{u}_i$ in the transport Eq. (5) and using the microscopic momentum equation for the material to find

$$\frac{\partial}{\partial t}(\theta_i \langle \rho_i^0 \rangle \tilde{\boldsymbol{u}}_i) + \nabla \cdot (\theta_i \langle \rho_i^0 \rangle \tilde{\boldsymbol{u}}_i \tilde{\boldsymbol{u}}_i) = \theta_i \langle \nabla \cdot \boldsymbol{\sigma}_i \rangle + \nabla \cdot (\theta_i \boldsymbol{\sigma}_i^{Re}) + \int \dot{C}_i \rho_i^0 \boldsymbol{u}_i \mathrm{d}\mathscr{P}, \tag{11}$$

where

$$\boldsymbol{\sigma}_i^{Re} = -\langle \rho_i^0 (\boldsymbol{u}_i - \tilde{\boldsymbol{u}}_i)(\boldsymbol{u}_i - \tilde{\boldsymbol{u}}_i) \rangle, \tag{12}$$

is the Reynolds stress resulting from velocity fluctuations. To further study the averaged momentum equation we introduce an auxiliary macroscopic stress field $\boldsymbol{\sigma}_{\mathrm{A}i}(\boldsymbol{x}, t)$ defined for phase i. In different fields related to multiphase flows the choice of this auxiliary stress is different as we will discuss later. For any such stress the first term on the right hand side of (11) can be written as

$$\theta_i \langle \nabla \cdot \boldsymbol{\sigma}_i \rangle = \theta_i \nabla \cdot \boldsymbol{\sigma}_{\mathrm{A}i} + \nabla \cdot [\theta_i (\langle \boldsymbol{\sigma}_i \rangle - \boldsymbol{\sigma}_{\mathrm{A}i})] + \boldsymbol{f}_i, \tag{13}$$

where

$$\boldsymbol{f}_i = -\int (\boldsymbol{\sigma}_i - \boldsymbol{\sigma}_{\mathrm{A}i}) \cdot \nabla C_i \mathrm{d}\mathscr{P}. \tag{14}$$

Substituting (13) into the momentum Eq. (11) one finds

$$\frac{\partial}{\partial t}(\theta_i \langle \rho_i^0 \rangle \tilde{\boldsymbol{u}}_i) + \nabla \cdot (\theta_i \langle \rho_i^0 \rangle \tilde{\boldsymbol{u}}_i \tilde{\boldsymbol{u}}_i) = \theta_i \nabla \cdot \boldsymbol{\sigma}_{\mathrm{A}i} + \nabla \cdot [\theta_i (\langle \boldsymbol{\sigma}_i \rangle - \boldsymbol{\sigma}_{\mathrm{A}i})] + \nabla \cdot (\theta_i \boldsymbol{\sigma}_i^{Re}) + \boldsymbol{f}_i + \int \dot{C}_i \rho_i^0 \boldsymbol{u}_i \mathrm{d}\mathscr{P}. \tag{15}$$

The interfacial force $\boldsymbol{f}_i$ defined in (14) depends on the choice of the macroscopic stress field $\boldsymbol{\sigma}_{\mathrm{A}i}$. The sum of the interfacial force is

$$\sum_{i=1}^{M} \boldsymbol{f}_i = -\int \sum_{i=1}^{M} \boldsymbol{\sigma}_i \cdot \nabla C_i \mathrm{d}\mathscr{P} + \sum_{i=1}^{M} \boldsymbol{\sigma}_{\mathrm{A}i} \cdot \nabla \theta_i. \tag{16}$$

The first term in (16) represents the effects of normal stress jumps, such as the surface tension, and is independent of the choice of the stress $\boldsymbol{\sigma}_{\mathrm{A}i}$. In the studies of two-phase flow in porous media (Bentsen, 2003), the stress is chosen to be the average stress of the phases, ($\boldsymbol{\sigma}_{\mathrm{A}i} = \langle \boldsymbol{\sigma}_i \rangle$). All choices are allowed provided that the interfacial forces defined in (14) are modeled accordingly, although some choices may facilitate or complicate closure development for a given practical problem. For instance, for a particle suspension under gravity, one can choose $\boldsymbol{\sigma}_{\mathrm{A}i}$ to be zero for the particle phase, as long as the model for the interfacial force $\boldsymbol{f}_i$ includes effects of buoyancy.

A typical choice for the stress $\boldsymbol{\sigma}_{\mathrm{A}i}$ in disperse multiphase flows is $\boldsymbol{\sigma}_{\mathrm{A}i} = \langle \boldsymbol{\sigma}_{\mathrm{c}} \rangle$, ($i = 1, \cdots, M$) where $\langle \boldsymbol{\sigma}_{\mathrm{c}} \rangle$ is the average stress for the continuous phase. With this choice, under the assumption that the particle size is small compared to the macroscopic length scale, the averaged momentum Eq. (15) can be written in the form derived by Zhang and Prosperetti (1994), Zhang and Prosperetti (1997) as shown in Appendix B. Studying one-dimensional Rayleigh–Taylor mixing, Glimm et al. (1999), and Saltz et al. (2000) introduced a

two-pressure model in which $\boldsymbol{\sigma}_{Ai} = \mathbf{0}$ and the interfacial terms are modeled as proportional to $\nabla\theta_i$. For instance, $\boldsymbol{f}_i$ is modeled as $p_i^*\nabla\theta_i$, where p_i^* is the pressure for phase i averaged on the interface. The gradient in the volume fraction provides a natural length scale for the interfacial force. Apparently these models are specifically devised for the Rayleigh–Taylor mixing problems, where the length scale in the problem is dominated by the length scale represented by the inverse of the volume fraction gradient, and cannot be extended easily to more general cases since the interfacial force is not necessarily zero when the gradient of the volume fraction vanishes.

Depending on the choice of $\boldsymbol{\sigma}_{Ai}$, the averaged stress differences may or may not appear explicitly in the momentum equations, but their effects are important from the point of view of multiphase flow theory. The stress difference (related to the stress $\boldsymbol{T}$ in Appendix B) is not only related to important quantities, such as effective viscosity in a Stokes flow (Zhang and Prosperetti, 1997), but also related to the characteristics of the averaged equations (Prosperetti, 1999). However, in many numerical calculations of disperse two-phase flows, especially for small particle volume fractions, the effect of the stress difference is neglected together with the Reynolds stresses and the particle collision stress (Pan et al., 2000; Zhang and VanderHeyden, 2001). When fine numerical meshes are used, such calculations can still produce results comparable to physical experiments. This is seemingly contradictory to the previous statements about the importance of the stress difference between the phases and can be explained by the effects of mesoscale structures in the multiphase flows. For disperse two-phase flows with the particle scale small compared to the macroscopic length scale of the flow, mesoscale structures often exist in the flow. Using a similar technique of deriving the averaged equations for disperse two-phase flows, one can average the averaged equations again over the mesoscale (Zhang and VanderHeyden, 2002). A similar stress difference term representing the stress difference inside and outside of the mesoscale structures appears in the double-averaged equations (see Eqs. (17)–(20) in that paper). The effect of the average stress difference between the particle phase and continuous phase is overwhelmed by the stress difference inside and outside of the mesoscale structures. In other words, the stress differences between different entities (between particles and continuous fluids or between inside and outside of mesoscale structures) in the flow are always important but they manifest themselves at different scales. When fine numerical meshes are used, the effects of the stress difference inside and outside the mesoscale structures are accounted for because the mesoscale structures are resolved in the calculation.

For continuous multiphase flows, different phases occupy regions of all scales, the double-averaging method cannot be applied. For these flows, the concepts, such as drag and added mass forces, need to be reconsidered, if they can be meaningfully defined. Their relations to the interfacial force $\boldsymbol{f}_i$ also need to be reexamined. Furthermore, for continuous multiphase flows, one has to explicitly consider the stress difference or average stresses of the all phases.

3. Continuity constraint on volumetric deformation models

The average stress of the material is often directly related to the average deformation gradient or average velocity gradient $\langle\nabla\boldsymbol{u}_i\rangle$ of the material. The average velocity gradient is not a primary variable in the averaged equation system, but can be related to the gradient of the average velocity by using (4),

$$\theta_i\langle\nabla\boldsymbol{u}_i\rangle = \theta_i\nabla\langle\boldsymbol{u}_i\rangle - \int(\boldsymbol{u}_i - \langle\boldsymbol{u}_i\rangle)\nabla C_i \mathrm{d}\mathscr{P}. \tag{17}$$

Therefore to calculate the stress in multiphase flows, a closure to the interface integral in the last term of (17) needs to be specified. The integral is a tensor. In this paper we focus on the study of the trace of this integral and leave the study of the closure for the deviatoric components of the integral to the future. This choice is based on the reason that the trace of this integral is related to the trace of $\langle\nabla\boldsymbol{u}_i\rangle$ and the pressure and temperature of the phase. In many high speed flows, the inertia, and therefore the pressure, dominate the motion of the system and the deviatoric stress can be neglected. The continuity condition provides a constraint on possible closures of the integral. To understand the consequence of this constraint is the main objective of this paper. We show that there is a family of possible closures for the integral and the equilibrium pressure model used in many calculations is one of the possible closures satisfying the constraint.

In many computations of multiphase flows, the volume fractions and the microscopic densities are not computed directly from the evolution equations, rather they are calculated as follows. The macroscopic density $\rho_i = \theta_i \langle \rho_i^0 \rangle$ is calculated using (7) with the velocity obtained from the momentum equations of the system. The average microscopic density is determined by finding an average pressure $\langle p_i \rangle$ according to the averaged equation of state for phase i such that the following equation is satisfied.

$$\sum_{i=1}^{M} \frac{\rho_i}{\langle \rho_i^0 \rangle (\langle p_i \rangle)} = \sum_{i=1}^{M} \theta_i = 1. \tag{18}$$

Eq. (18) contains M unknown pressures, $M-1$ additional relations are needed to solved it. The simplest and most commonly used assumption is the equilibrium pressure assumption ($\langle p_i \rangle = p$). Regardless of the assumptions or the numerical methods used to solve this equation, if models for the phase change terms in (9) and (10) are specified, any method that provides a way to determine the volume fraction and the microscopic density is equivalent to making closure assumptions about the interface integral $\int (\boldsymbol{u}_i - \tilde{\boldsymbol{u}}_i) \cdot \nabla C_i \mathrm{d}\mathscr{P}$ in the last terms on the right hand sides of the equations. We now study the constraint for the closures of this interface integral; and then use the constraint to guide us to a model that allows different pressures for different phases.

From (17) we find

$$\int (\boldsymbol{u}_i - \tilde{\boldsymbol{u}}_i) \nabla C_i \mathrm{d}\mathscr{P} = \theta_i (\nabla \tilde{\boldsymbol{u}}_i - \langle \nabla \boldsymbol{u}_i \rangle) - \nabla (\theta_i \langle \rho_i^{0\prime} \boldsymbol{u}_i' \rangle / \langle \rho_i^0 \rangle), \tag{19}$$

after using $\tilde{\boldsymbol{u}}_i - \langle \boldsymbol{u}_i \rangle = \langle \rho_i^{0\prime} \boldsymbol{u}_i' \rangle / \langle \rho_i^0 \rangle$, where $\boldsymbol{u}_i' = \boldsymbol{u}_i - \langle \boldsymbol{u}_i \rangle$ and $\rho_i^{0\prime} = \rho_i^0 - \langle \rho_i^0 \rangle$ are the fluctuation components of the velocity and the microscopic material density ρ_i^0. In many multiphase flows, the last term in (19) can be neglected. For instance, if the density fluctuations are caused by pressure fluctuations, p_i', then using the equation of state we have $\rho_i^{0\prime} = p_i'/c_i^2$, where c_i is the speed of sound for phase i. After using the momentum equation for the material, we find p_i' (due to the Bernoulli effect) is of order $\langle \rho_i^0 \rangle \langle \boldsymbol{u}_i \rangle \cdot \boldsymbol{u}_i'$, and the last term in Eq. (19) can be estimated as $\mathrm{O}(\theta_i \langle \boldsymbol{u}_i \rangle \boldsymbol{u}_i' \cdot \boldsymbol{u}_i'/c_i^2)$. If the fluctuation velocity is small compared to the sound speed, which is true for many practical cases of multiphase flows, the last term of (19) can be neglected. There are cases, such as Rayleigh–Benard convection, in which the correlation between the velocity fluctuation and the microscopic density cannot be neglected. In this paper we restrict ourselves to the cases where the correlation $\langle \rho_i^{0\prime} \boldsymbol{u}_i' \rangle$ is negligible. Under this restriction Eq. (19) implies that a closure for $\int (\boldsymbol{u}_i - \tilde{\boldsymbol{u}}_i) \nabla C_i \mathrm{d}\mathscr{P}$ provides a relation between the gradient of the average velocity $\nabla \tilde{\boldsymbol{u}}_i$ and the average of the velocity gradient $\langle \nabla \boldsymbol{u}_i \rangle$ of the material.

Closures of the interface integral cannot be arbitrary. They are constrained by the microscopic continuity condition,

$$\sum_{i=1}^{M} \frac{\partial C_i}{\partial t} = 0. \tag{20}$$

Using this condition, we find the constraint for the closure after using (2) and (6).

$$\sum_{i=1}^{M} \int (\boldsymbol{u}_i - \tilde{\boldsymbol{u}}_i) \cdot \nabla C_i \mathrm{d}\mathscr{P} = \sum_{i=1}^{M} \left(\int \dot{C}_i \mathrm{d}\mathscr{P} - \tilde{\boldsymbol{u}}_i \cdot \nabla \theta_i \right). \tag{21}$$

This constraint (21) on the closure relation is equivalent to the requirement of (18) because, by differentiating (18) and using (10), we have

$$\frac{\partial}{\partial t} \sum_{i=1}^{M} \frac{\rho_i}{\langle \rho_i^0 \rangle} = -\sum_{i=1}^{M} \left[\int (\boldsymbol{u}_i - \tilde{\boldsymbol{u}}_i) \cdot \nabla C_i \mathrm{d}\mathscr{P} + \tilde{\boldsymbol{u}}_i \cdot \nabla \theta_i - \int \dot{C}_i \mathrm{d}\mathscr{P} \right]. \tag{22}$$

If (21) is satisfied, we have $\frac{\partial}{\partial t} \sum_{i=1}^{M} \theta_i = 0$. If the initial volume fractions of all the phases sum to one, it remains one during the system evolution. Conversely, if (18) is satisfied, the left hand side of (22) vanishes and (21) is satisfied.

Either Eq. (18) or (21) provides a constraint on closures for the interface integral, $\int (\boldsymbol{u}_i - \tilde{\boldsymbol{u}}_i) \cdot \nabla C_i \mathrm{d}\mathscr{P}$, but does not specify a model for this integral for each individual phase. For an incompressible phase i, $\nabla \cdot \boldsymbol{u}_i = 0$. Upon substitution of this into (19) we find the closure for the interface integral,

$$\int (\boldsymbol{u}_i - \tilde{\boldsymbol{u}}_i) \cdot \nabla C_i \mathrm{d}\mathscr{P} = \theta_i \nabla \cdot \tilde{\boldsymbol{u}}_i, \tag{23}$$

because the microscopic material density ρ_i^0 is constant, and the last term of (19) vanishes.

In the case where all the phases are incompressible, without phase changes, the constraint (21) or (23) leads to the familiar continuity condition for the mixture

$$\nabla \cdot \sum_{i=1}^{M} \theta_i \tilde{\boldsymbol{u}}_i = 0. \tag{24}$$

It is known that this constraint on the average velocities is equivalent to (18) for multiphase flows when all phases are incompressible.

For compressible phases, the interface integral needs to be modeled. The models for the integral are not unique. In the next section we first show the implied model for the interface integral under the equilibrium pressure assumption, then propose another model in the following section. The purpose of this work is not to advocate one model over the other, but rather to show their advantages and disadvantages when used in different circumstances.

4. Equilibrium pressure assumption

Under the equilibrium pressure assumption all phases have the same pressure. This assumption is often generalized as that the time derivatives of the pressures are the same for all the phases ($\partial\langle p_i\rangle/\partial t = \partial p/\partial t$) to accommodate the effect of surface tension.

By differentiating (18) and using (7) we find

$$\frac{\partial p}{\partial t} = \sum_{i=1}^{M} \frac{1}{\langle \rho_i^0 \rangle} \left[\int \rho_i^0 \dot{C}_i \mathrm{d}\mathscr{P} - \nabla \cdot (\theta_i \langle \rho_i^0 \rangle \tilde{\boldsymbol{u}}_i) \right] \Big/ \sum_{i=1}^{M} \frac{\theta_i}{c_i^2 \langle \rho_i^0 \rangle}, \tag{25}$$

where

$$c_i^2 = \frac{\partial \langle p_i \rangle}{\partial \langle \rho_i^0 \rangle}. \tag{26}$$

Here c_i is different from the speed of sound of the material. By expanding the equation of state in the vicinity of the average density and the average temperature, after averaging, one finds that the averaged equation of state differs from the original equation of state for the material by quadratic terms in density and temperature fluctuations. If these fluctuations result from velocity fluctuations, similar to the analysis following (19), using the momentum and energy equations for the material, one can estimate that these quadratic terms are negligible for flows in which Mach number of the fluctuation velocity is small. Under this assumption, c_i defined in (26) can be approximated by the speed of sound of the material.

Using (26) we have

$$\frac{\partial \langle \rho_i^0 \rangle}{\partial t} = \frac{1/c_i^2}{\sum_{i=1}^{M} \theta_i / (c_i^2 \langle \rho_i^0 \rangle)} \sum_{i=1}^{M} \frac{1}{\langle \rho_i^0 \rangle} \left[\int \rho_i^0 \dot{C}_i \mathrm{d}\mathscr{P} - \nabla \cdot (\theta_i \langle \rho_i^0 \rangle \tilde{\boldsymbol{u}}_i) \right]. \tag{27}$$

Substituting (27) into (10), one finds

$$\begin{aligned} \int (\boldsymbol{u}_i - \tilde{\boldsymbol{u}}_i) \cdot \nabla C_i \mathrm{d}\mathscr{P} = {} & \frac{\theta_i / (c_i^2 \langle \rho_i^0 \rangle)}{\sum_{i=1}^{M} (\theta_i / c_i^2 \langle \rho_i^0 \rangle)} \sum_{i=1}^{M} \frac{1}{\langle \rho_i^0 \rangle} \left[\int \rho_i^0 \dot{C}_i \mathrm{d}\mathscr{P} - \nabla \cdot (\theta_i \langle \rho_i^0 \rangle \tilde{\boldsymbol{u}}_i) \right] \\ & + \frac{\theta_i \nabla \cdot (\langle \rho_i^0 \rangle \tilde{\boldsymbol{u}}_i)}{\langle \rho_i^0 \rangle} - \frac{1}{\langle \rho_i^0 \rangle} \int (\rho_i^0 - \langle \rho_i^0 \rangle) \dot{C}_i \mathrm{d}\mathscr{P}(\mathscr{F}). \end{aligned} \tag{28}$$

If we further assume that the pressure gradients for all the phases are also the same, using (26) to $\nabla \cdot (\theta_i \langle \rho_i^0 \rangle \tilde{\boldsymbol{u}}_i)$ in the right hand side of (25) we can rewrite (25) as

$$\frac{\partial p}{\partial t}+\boldsymbol{u}_{\mathrm{s}}\cdot\nabla p=\sum_{i=1}^{M}\left[\frac{1}{\langle\rho_i^0\rangle}\int\rho_i^0\dot{C}_i\mathrm{d}\mathscr{P}-\nabla\cdot(\theta_i\tilde{\boldsymbol{u}}_i)\right]\Big/\sum_{i=1}^{M}\frac{\theta_i}{c_i^2\langle\rho_i^0\rangle}, \tag{29}$$

where $\boldsymbol{u}_{\mathrm{s}}$ is the sonic average velocity (Kashiwa and Rauenzahn, 1994) defined as

$$\boldsymbol{u}_{\mathrm{s}}=\frac{\sum_{i=1}^{M}\theta_i\tilde{\boldsymbol{u}}_i/(c_i^2\langle\rho_i^0\rangle)}{\sum_{i=1}^{M}\theta_i/(c_i^2\langle\rho_i^0\rangle)}. \tag{30}$$

This closure for $\int(\boldsymbol{u}_i-\tilde{\boldsymbol{u}}_i)\cdot\nabla C_i\mathrm{d}\mathscr{P}$, or equivalently Eq. (27) implies that the local microscopic density change is not directly related to the velocity field of the individual phase, but related to the mixture motion. For a disperse multiphase flow, if the typical size of the particles is small compared to the macroscopic length scale of the flow, it is true that the microscopic density change of the disperse phase is not directly related to its velocity field. On the other hand, for the continuous phases one expects a more direct relation between the microscopic density change and the velocity field of the phase. Clearly it is advantageous to have a more flexible relation between the microscopic density changes and the velocity fields for both the disperse and continuous phases. The multipressure model described in the next section provides such flexibility.

5. A multipressure model

We note that $\int(\boldsymbol{u}_i-\tilde{\boldsymbol{u}}_i)\cdot\nabla C_i\mathrm{d}\mathscr{P}$ represents the difference between $\langle\nabla\cdot\boldsymbol{u}_i\rangle$ and $\nabla\cdot\tilde{\boldsymbol{u}}_i$, if the last term in (19) is negligible as we always assume in this paper. To accommodate a more flexible relation between $\langle\nabla\cdot\boldsymbol{u}_i\rangle$ and $\nabla\cdot\tilde{\boldsymbol{u}}_i$ for different phases as mentioned in the previous section we introduce a coefficient α_i for each phase and write

$$\langle\nabla\cdot\boldsymbol{u}_i\rangle=\alpha_i\nabla\cdot\tilde{\boldsymbol{u}}_i+B_i. \tag{31}$$

Evidently, the coefficient α_i introduced here is related to the connectivity or morphology, material properties, and volume fraction of the phase. For continuous multiphase flows, satisfactory results can often be found by simply assuming $\alpha_i=\theta_i$, or $\alpha_i=1$ if the volume fraction is sufficiently large (>90%) or the phase is well connected. The term B_i is introduced to allow for deficiencies in the modeling by the first term alone. Using (31) and (19) we have

$$\int(\boldsymbol{u}_i-\tilde{\boldsymbol{u}}_i)\cdot\nabla C_i\mathrm{d}\mathscr{P}=\theta_i[(1-\alpha_i)\nabla\cdot\tilde{\boldsymbol{u}}_i-B_i]. \tag{32}$$

If phase i is incompressible, comparing (32) to (23) we find $\alpha_i=0$ and $B_i=0$.

Using (32), Eq. (9) can be written as

$$\frac{\partial\theta_i}{\partial t}+\nabla\cdot(\theta_i\tilde{\boldsymbol{u}}_i)=\alpha_i\theta_i\nabla\cdot\tilde{\boldsymbol{u}}_i+\int\dot{C}_i\mathrm{d}\mathscr{P}+\theta_iB_i, \tag{33}$$

and (10) can be written as

$$\theta_i\frac{\mathrm{d}\langle\rho_i^0\rangle}{\mathrm{d}t}=-\theta_i\langle\rho_i^0\rangle[\alpha_i\nabla\cdot\tilde{\boldsymbol{u}}_i+B_i]+\int\left(\rho_i^0-\langle\rho_i^0\rangle\right)\dot{C}_i\mathrm{d}\mathscr{P}. \tag{34}$$

To ensure that the volume fraction of all the phases sum to one, or equivalently for $\int(\boldsymbol{u}_i-\tilde{\boldsymbol{u}}_i)\cdot\nabla C_i\mathrm{d}\mathscr{P}$ to satisfy (21), quantity B_i satisfies

$$\sum_{i=1}^{M}\theta_iB_i=\sum_{i=1}^{M}\left[\nabla\cdot(\theta_i\tilde{\boldsymbol{u}}_i)-\alpha_i\theta_i\nabla\cdot\tilde{\boldsymbol{u}}_i-\int\dot{C}_i\mathrm{d}\mathscr{P}\right]. \tag{35}$$

This equation does not uniquely determine B_i for all the phases. To uniquely determine B_i, we assume the pressure increase $\partial p_i/\partial t$ caused by B_i for all the phases is the same. For example, one may consider $\partial p_i/\partial t$ to be due to the propagation of fast pressure waves in the system, while the underlying non-equilibrium state would need

much slower convective time scale to equilibrate. Using this assumption, (34) and the equation of state (26) we have

$$\langle \rho_i^0 \rangle c_i^2 B_i = -\partial p_a / \partial t, \tag{36}$$

where $\partial p_a/\partial t$ is the same for all the phases. Solving Eqs. (36) and (35) we find

$$B_i = \frac{1/(\langle \rho_i^0 \rangle c_i^2)}{\sum_{i=1}^N \theta_i/(\langle \rho_i^0 \rangle c_i^2)} \sum_{i=1}^M \left[\nabla \cdot (\theta_i \tilde{\boldsymbol{u}}_i) - \alpha_i \theta_i \nabla \cdot \tilde{\boldsymbol{u}}_i - \int \dot{C}_i \mathrm{d}\mathscr{P} \right], \tag{37}$$

and

$$\int (\boldsymbol{u}_i - \tilde{\boldsymbol{u}}_i) \cdot \nabla C_i \mathrm{d}\mathscr{P} = (1-\alpha_i)\theta_i \nabla \cdot \tilde{\boldsymbol{u}}_i - \frac{\theta_i/(\langle \rho_i^0 \rangle c_i^2)}{\sum_{i=1}^N \theta_i/(\langle \rho_i^0 \rangle c_i^2)} \sum_{i=1}^M \left[\nabla \cdot (\theta_i \tilde{\boldsymbol{u}}_i) - \alpha_i \theta_i \nabla \cdot \tilde{\boldsymbol{u}}_i - \int \dot{C}_i \mathrm{d}\mathscr{P} \right], \tag{38}$$

after using (32).

With the closure for $\int (\boldsymbol{u}_i - \tilde{\boldsymbol{u}}_i) \cdot \nabla C_i \mathrm{d}\mathscr{P}$ explicitly given in (28) under the equilibrium pressure assumption or in (38) with the multipressure model introduced in this section, the volume fractions and microscopic densities for all the phases can be calculated from evolution equations (9) and (10) and Eq. (18) is redundant because both closures (28) and (38) satisfy constraint (21), which is equivalent to (18) as proved in Section 2 provided that the initial volume fractions sum to one. In this way one can avoid solving (18), which is typically nonlinear and requires an implicit method. This implementation of the closures can reduce the amount of calculation and could be significant in an explicit numerical scheme. However there is a shortcoming with this implementation and it should be used with care. Since this explicit scheme enforces $\sum_{i=1}^M \partial \theta_i/\partial t = 0$ at every time step, instead of $\sum_{i=1}^M \theta_i = 1$, error accumulation over time may result with the sum of the volume fractions noticeably deviating from one, especially in cases with large Courant numbers and a large number of time steps.

To avoid this possible numerical error, we now introduce another numerical implementation of the multipressure model that solves Eq. (18). This method can be viewed as a modification to the traditional predictor–corrector method used with the equilibrium pressure assumption. As in the traditional pressure calculation, the macroscopic densities $\rho_i = \theta_i \langle \rho_i^0 \rangle$ in the numerators of (18) are calculated from the transport Eq. (7). After obtaining ρ_i, instead of using the equations of state for all the phases to find a common pressure p to satisfy (18), we advance θ_i with the chosen α_i as if the last term $\theta_i B_i$ in (33) were absent to obtain an interim volume fraction θ_i^*. Using this interim volume fraction, θ_i^*, an interim microscopic density, $\langle \rho_i^0 \rangle^* = \rho_i/\theta_i^*$, and the corresponding pressure p_i^*, such that $\langle \rho_i^0 \rangle^* = \rho_i^0(p_i^*)$ can be calculated. Such calculated ρ_i and $\langle \rho_i^0 \rangle^*$ do not satisfy (18) in general. The final values of averaged microscopic densities, $\langle \rho_i^0 \rangle = \rho_i^0(p_i^* + \Delta p)$, are obtained by finding a common pressure increase, Δp, satisfying (18), that is

$$\sum_{i=1}^M \frac{\rho_i}{\rho_i^0(p_i^* + \Delta p)} = 1. \tag{39}$$

In this way, we do not directly use (37), instead we use the assumption (36) to find $\Delta p = (\partial p_a/\partial t)\Delta t$, which implies (37).

The use of (39) has an additional advantage in the case where all the phases are incompressible. In such cases ρ_i^0 in (39) is independent of Δp, but the numerator ρ_i is a function of Δp in an implicit numerical scheme. Therefore the pressure increase can still be determined. In this case, the pressure increment is the same at every time step for all the phases, therefore the pressures for all the incompressible phases are the same provided their initial pressures are the same.

For an incompressible phase i, in the absence of phase change, if we use the equilibrium pressure model, the closure (28) for the interface phase integral $\int (\boldsymbol{u}_i - \tilde{\boldsymbol{u}}_i) \cdot \nabla C_i \mathrm{d}\mathscr{P}$ leads to the evolution equation for the microscopic density

$$\frac{\partial \langle \rho_i^0 \rangle}{\partial t} = 0, \tag{40}$$

while the multipressure model leads to

$$\frac{\mathrm{d}\langle\rho_i^0\rangle}{\mathrm{d}t} = \frac{\partial\langle\rho_i^0\rangle}{\partial t} + \tilde{\boldsymbol{u}}_i \cdot \nabla\langle\rho_i^0\rangle = 0, \tag{41}$$

since $\alpha_i = 0$ and $B_i = 0$ in (34).

Finally, we note that for cases, such as slow expansion of uniformly distributed large gas bubbles in a compressible viscous fluid in a closed container without macroscopic motion ($\nabla \cdot \tilde{\boldsymbol{u}}_i = 0$), an additional model term,

$$\sum_{j=1}^{M} \frac{\theta_j}{\tau_{ij}} \frac{(p_j - p_i)}{\sqrt{\langle\rho_i^0\rangle\langle\rho_j^0\rangle}c_i c_j},$$

to (31) is needed, (with corresponding changes in (32), (33), (34) and (38)), to account for the process of pressure equilibration among the phases due to exchange of volume among them, where the $\tau_{ij}(=\tau_{ji})$ is a time scale for pressure equilibration. In the example that follows, we will assume the equilibration time scales are very long compared to the dynamics and this term will therefore be neglected. We include it here, however, for completeness and to show how the multipressure model can include the case of pressure equilibration.

6. A numerical example

The use of an equilibrium pressure model has become a standard practice in the computation of multiphase flows (Sundaresan, 2000). In this section we use a numerical example to examine the properties of the multipressure model.

We consider the tensile failure, known as spalling, resulting from the collision of two porous elastic plates with thickness L and $2L$. It is well known that the pressure for the gas phase always stays positive. If the equilibrium pressure model were used the pressure (or the negative of the trace of the stress) in the solid material would be the same as the gas pressure; the solid material would always be in the state of compression and spalling would never happen. Therefore to simulate the spalling phenomenon, one has to use a multipressure model. As indicated in the derivation of the multipressure model many multipressure models are possible. The multipressure model introduced in the last section is one of such candidates and is used in the calculation described in this section.

At time $t = 0$ the thinner plate with velocity V collides with the thicker plate at rest with the presence of air inside and outside the plates. Physically, the presence of the air has a negligible effect on the collision process if the solid material has a density significantly larger than that of the air. However, to have a computational model with the ability to simultaneously calculate the air flow and the solid deformation is a significant challenge and has important applications, for instance, in the explosion process of a tank filled with compressed air. The break-up of the tank and the subsequent trajectories of the tank fragments are of practical interest to many safety engineers and bomb designers. The plate collision example in this paper is chosen to demonstrate the new capability enabled by the multipressure model introduced in this paper. If the effect of the air is neglected, there is an analytical representation of the collision process. In the case where the air is present, we expect that the numerical solution obtained using the multipressure model to be close to the analytical solution without accounting for the effect of the air, therefore the analytical solution provides a point of reference to our numerical scheme and physical model.

At the moment when the moving thinner plate impacts the thicker plate at rest, stress waves are generated and travel in both directions from the impact surface. If the thickness of the plate is small compared to the other two dimensions of the plate, the elastic waves can be approximated as plane waves with wave speed $c_\mathrm{e} = \sqrt{E/\rho_\mathrm{e}^0}$, where E is the Young's modulus of the plate material and ρ_e^0 is the microscopic density of the elastic material. Since both plates are made of the same material, the speeds c_e of the stress waves in both directions are the same. In the time interval Δt, the waves travel distance $c_\mathrm{e}\Delta t$ and change the velocity in the material experiencing the stress waves in both directions. Using the principle of momentum conservation, we find the velocity in the region visited by the stress waves to be $V/2$ and the impulse in the time interval to be

$$I = c_\mathrm{e}\Delta t A \rho_\mathrm{e}^0 V/2 = \sigma A \Delta t, \tag{42}$$

where σ is the stress in the elastic body and A is the area of the plate. The stress σ can be solved from (42)

$$\sigma = c_e \rho_e^0 V/2 = \sqrt{\rho_e^0 E}\, V/2. \tag{43}$$

The waves generated on the impact surface are compression waves, when they reach both ends of the plates, they reflect back as tension waves. Since the waves travel at the same speed in both directions, the reflected waves meet at the middle plane of the thicker plate. When they meet, the stress in this location becomes 2σ in tension as the stress from both waves superpose. If the material tensile strength is between σ and 2σ, the thicker plate breaks at the middle plane, a phenomenon known as spalling.

In the numerical example, we set

$$E = 70\ \text{GPa}, \quad \rho_e^0 = 2700\ \text{kg/m}^3, \quad V = 100\ \text{m/s}. \tag{44}$$

The wave speed in the material is then $c_e = 5.09$ km/s and the stress $\sigma = 0.687$ GPa. The tensile strength of the elastic material is set to be $\sigma_T = 1.0$ GPa, about the middle point of the stresses σ and 2σ.

The density of air at atmospheric pressure is about 1.2 kg/m^3. In the calculation, the air is regarded as an ideal gas. In this example the density ratio of the solid to the gas is more than 2000.

A two-dimensional calculation was performed on a rectangular region of 1.5 cm by 1.0 cm. On the boundaries the normal velocities are set to be zero. Initially, the thickness of the thinner plate is $L = 0.2$ cm with the bottom located at $y = 0.7$ cm in the computational domain. In the x-direction the plate spans from 0.1 cm to 1.4 cm in the computational domain. Initially, the thickness of the thicker plate is $2L = 0.4$ cm, with top located at $y = 0.7$ cm in the computational domain. The initial porosity (or the air volume fraction) in the plates is 1%. The initial velocity of the thinner plate is -100 m/s while the velocity of the thicker plate is zero. In the numerical calculation, the coefficient α_i in (31) is set to one for both phases, to ensure the maximum correlation between $\langle \nabla \cdot \boldsymbol{u}_i \rangle$ and $\nabla \cdot \tilde{\boldsymbol{u}}_i$; and B_i is determined by solving Eq. (39). We apply a simple material failure model, in which when the maximum principal stress exceeds the tensile strength σ_T, the stress in the principal direction is set to zero and the material at the location is marked as damaged.

According to the elastic wave speed, one can predict that the time for the two reflected tension waves to meet at the middle plane is 1.18 μs after impact. Our numerical calculation finds that the first damage occurs at time 1.12 μs and is located at the middle of the plate. Fig. 1. shows the damage of the material 2 μs after the impact. The damaged material is colored red and undamaged is marked blue.

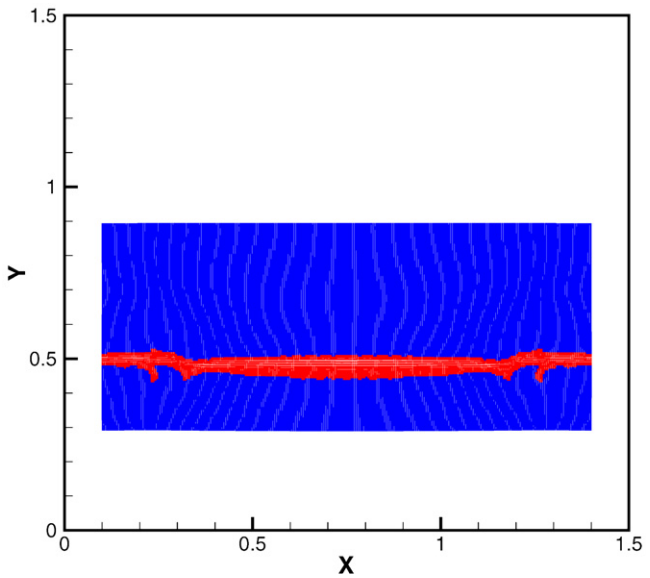

Fig. 1. Spall of an elastic plate. The area damaged by tensile stress is marked red.

7. Conclusions

The difference between the average volumetric deformation rate and the divergence of the average velocity is proved to be the interface integral $\int(\boldsymbol{u}_i - \tilde{\boldsymbol{u}}_i)\cdot\nabla C_i \mathrm{d}\mathscr{P}$. Any method of calculating pressures in a multiphase flow is equivalent to a closure of the interface integral because the volumetric deformation is related to the pressure of the phase. Continuity of the multiphase system provides a constraint to the closure. However this constraint is not sufficient to determine the closures for the interface integrals for all the phases; therefore different closure models or pressure models are possible. The traditionally used equilibrium pressure model is one of the models that satisfy the continuity constraint. Application of the equilibrium pressure model to continuous multiphase flows has been shown to encounter a conceptual difficulty and multipressure models have to be introduced as an alternative. In the multipressure model introduced in the present paper, the interface integral is written as a summation of two terms. The first term is proportional to the divergence of the average phase velocity with a coefficient expected to be a function of the volume fractions and morphology of the multiphase system. The second term is related to the relative compressibilities of the phases. Pressure equilibration among the phases can also be included as a third term for problems in which this effect is important.

Numerical implementation of the multipressure model only requires a small modification of the codes implemented with equilibrium pressure models. While further evaluation of the multipressure model is needed, the numerical example in the present paper indicates the suitability of the model to problems where the volumetric deformation rate is strongly correlated to the divergence of the average velocity.

Acknowledgments

This work was performed under the auspices of the United States Department of Energy. The Stockpile Safety and Surety Program, the Joint DOD/DOE Munitions Technology Development Program and the ASC Program provided the financial support for this work.

Appendix A. Probability and average

Following statistical mechanics, Zhang and Prosperetti (1994), Zhang and Prosperetti (1997) derived averaged equations by averaging over an ensemble of two-phase flows. They used the Liouville equation in a phase space comprised of the positions and velocities of particles. For the potential and Stokes flows they treated, the motion of the continuous fluid is uniquely determined by the motions and positions of the particles; therefore the continuous fluid does not possess additional degrees of freedom, and the phase space has a finite dimension. This is no longer true for flows with finite Reynolds number, in which the degrees of freedom of the continuous fluid are infinite. Thus the concept of probability defined in a finite-dimensional phase space needs to be extended to handle these systems. For such an extension, we note that the probability of finding flows in a given subset of the ensemble is defined by the nature of the physics involved, and is independent of the parameters, or degrees of freedom, that we choose to describe them. This notion of parameter independence is similar to the notion of coordinate system independence in describing physical systems; different coordinate systems can be used to describe the same set of flows. In different descriptions of the flows, the phase space and the probability density are different, but the probability of finding flows belonging to the subset of the ensemble is independent of the description. The probability density defined in a phase space is merely a representation of the probability defined by the physical process. This description-independent probability can be used to treat systems with finite or infinite degrees of freedom, because degrees of freedom, finite or infinite, are merely descriptions of the system. This type of probability is common in real analysis and modern probability theory. Drew and Passman (1999) used this probability as a conceptual starting point to derive averaged equations for multiphase flows.

Following Drew and Passman, we now introduce a probability $\mathscr{P}$ defined on a collection of subsets of the flows in the ensemble Ω. A subset in the collection is called an event in probability theory. The probability is a set function that maps an event (a subset in the collection), to a real number between 0 and 1. To ensure that such a probability is well defined and has the properties with which we are already familiar, there are certain conditions that need to be satisfied by the set function and by the collection of the subsets. Almost all physical

systems of interest satisfy these conditions; therefore we do not list them here. Readers interested in more details are referred to textbooks on real analysis and probability theory, (e.g. Ash, 1972). The focus of this Appendix is the connection between this probability and the probability density defined in the phase space used by Zhang and Prosperetti (1994), Zhang and Prosperetti (1997) in the derivation of the averaged equations. This connection is particularly useful because the probability defined on the collection of subsets is quite abstract and difficult to manipulate. The probability defined in the phase space, although not as general, is easy to apply. For instance, the small particle approximation (Zhang and Prosperetti, 1994, 1997) can only be obtained by using the probability density defined on particle configurations as derived in the following.

The average of function, f, which depends on a spatial position $\boldsymbol{x}$, time t and flow $\mathscr{F}$ in the ensemble, is the probability integral (associated with the probability measure) over all possible flows in the ensemble, and is denoted as $\int f(\boldsymbol{x},t,\mathscr{F})\mathrm{d}\mathscr{P}$. Here, we assume that all the functions of interest satisfy the integrability condition under the probability $\mathscr{P}$ (Yosida, 1966; Ash, 1972). For such a probability to be useful we further assume that differentiation with respect to both position $\boldsymbol{x}$ and time t can be exchanged freely with the probability integral for the functions of interest.

For a system with N particles at time t the probability density of finding a particle configuration $\mathscr{C}^N = \{\boldsymbol{x}_1,\ldots,\boldsymbol{x}_N;\boldsymbol{v}_1,\ldots,\boldsymbol{v}_N\}$ in which particle α is at a specified position $\boldsymbol{x}_\alpha$ with a specified velocity $\boldsymbol{v}_\alpha$ for $\alpha = 1,\ldots,N$ is related to the probability $\mathscr{P}$ as follows:

$$P(\mathscr{C}^N,t) = \int \delta[\boldsymbol{x}_1 - \boldsymbol{y}_1(\mathscr{F},t)]\cdots\delta[\boldsymbol{x}_N - \boldsymbol{y}_N(\mathscr{F},t)]\delta[\boldsymbol{v}_1 - \boldsymbol{w}_1(\mathscr{F},t)]\cdots\delta[\boldsymbol{v}_N - \boldsymbol{w}_N(\mathscr{F},t)]\mathrm{d}\mathscr{P}, \tag{45}$$

where $\boldsymbol{y}_\alpha(\mathscr{F},t)$ and $\boldsymbol{w}_\alpha(\mathscr{F},t)$ are the position and velocity of particle α in flow $\mathscr{F}$ at time t. In this definition the δ-functions select the flows with configuration $\mathscr{C}^N$ from the ensemble; and the integral averages over all the flows satisfying the configuration. The conditional average $\bar{q}(\boldsymbol{x},t|\mathscr{C}^N)$ of a quantity $q(\boldsymbol{x},t,\mathscr{F})$ given the configuration $\mathscr{C}^N$ can be calculated by averaging over all flows satisfying the configuration as

$$P(\mathscr{C}^N,t)\bar{q}(\boldsymbol{x},t|\mathscr{C}^N) = \int q(\boldsymbol{x},t,\mathscr{F})\delta[\boldsymbol{x}_1 - \boldsymbol{y}_1(\mathscr{F},t)]\cdots\delta[\boldsymbol{x}_N - \boldsymbol{y}_N(\mathscr{F},t)]\delta[\boldsymbol{v}_1 - \boldsymbol{w}_1(\mathscr{F},t)]\cdots\delta[\boldsymbol{v}_N - \boldsymbol{w}_N(\mathscr{F},t)]\mathrm{d}\mathscr{P}. \tag{46}$$

In particular, the conditionally averaged acceleration $\bar{\dot{\boldsymbol{v}}}_\alpha$ of particle α can be calculated by

$$P(\mathscr{C}^N,t)\bar{\dot{\boldsymbol{v}}}_\alpha(t|\mathscr{C}^N) = \int \dot{\boldsymbol{w}}_\alpha(\mathscr{F},t)\delta[\boldsymbol{x}_1 - \boldsymbol{y}_1(\mathscr{F},t)]\cdots\delta[\boldsymbol{x}_N - \boldsymbol{y}_N(\mathscr{F},t)]\delta[\boldsymbol{v}_1 - \boldsymbol{w}_1(\mathscr{F},t)]\cdots\delta[\boldsymbol{v}_N - \boldsymbol{w}_N(\mathscr{F},t)]\mathrm{d}\mathscr{P}. \tag{47}$$

By differentiating (45) with respect to time t and then using (46), we find a generalized Liouville equation,

$$\frac{\partial P}{\partial t} + \sum_{\alpha=1}^{N}[\nabla_{\boldsymbol{x}_\alpha}\cdot(\boldsymbol{v}_\alpha P) + \nabla_{\boldsymbol{v}_\alpha}\cdot(\bar{\dot{\boldsymbol{v}}}_\alpha P)] = 0, \tag{48}$$

where we have used $\nabla_{\boldsymbol{y}_\alpha}\delta(\boldsymbol{x}_\alpha - \boldsymbol{y}_\alpha) = -\nabla_{\boldsymbol{x}_\alpha}\delta(\boldsymbol{x}_\alpha - \boldsymbol{y}_\alpha)$ and $\nabla_{\boldsymbol{w}_\alpha}\delta(\boldsymbol{v}_\alpha - \boldsymbol{w}_\alpha) = -\nabla_{\boldsymbol{v}_\alpha}\delta(\boldsymbol{v}_\alpha - \boldsymbol{w}_\alpha)$, and exchanged differentiation with the probability integration. For systems that can be uniquely described by the particle configuration $\mathscr{C}^N$, the average sign (over-bar) for the acceleration $\bar{\dot{\boldsymbol{v}}}_\alpha$ is not necessary ($\bar{\dot{\boldsymbol{v}}}_\alpha = \dot{\boldsymbol{w}}_\alpha$), and Eq. (48) becomes the Liouville equation.

The probability density defined in (45) is for distinguishable particles, while the probability density P_{zp} used by Zhang and Prosperetti (1994), Zhang and Prosperetti (1997) is for indistinguishable particles. These two probabilities are connected simply by $P_{zp} = \sum P(\mathscr{C}^N,t)$, where the summation is over all $N!$ possible permutations of particle numberings. Therefore the probability density defined in (45) normalizes to one, while P_{zp} normalizes to $N!$. Using this connection, one can show that generalized Liouville Eq. (48) is also satisfied by P_{zp}. This result implies that probability used in the present paper is consistent with the probability used by Zhang and Prosperetti (1994), Zhang and Prosperetti (1997) for the cases they treated.

Because we have derived the generalized Liouville Eq. (48) and the transport Eq. (5) without referring to the phase space, the equations obtained by Zhang and Prosperetti (1994), Zhang and Prosperetti (1997) can be used in disperse multiphase flows with finite Reynolds numbers.

Appendix B. Small particle approximation

If the typical size of the disperse phase is small compared to the macroscopic length scale, the small particle approximation (Zhang and Prosperetti, 1997) can be made to the interfacial force. Under this approximation and with the choice $\boldsymbol{\sigma}_{\mathrm{A}i} = \langle \boldsymbol{\sigma}_{\mathrm{c}} \rangle$, $(i = 1, \cdots, M)$, where $\langle \boldsymbol{\sigma}_{\mathrm{c}} \rangle$ is the average stress for the continuous phase, one can write

$$\boldsymbol{f}_c = -\theta_{\mathrm{d}} \boldsymbol{F}_{\mathrm{d}} + \nabla \cdot (\theta_{\mathrm{d}} \boldsymbol{T}), \tag{49}$$

where $\boldsymbol{F}_{\mathrm{d}}$ is the force density with which the continuous phase acts on particles, and $\boldsymbol{T}$ is a stress tensor. In the case of spherical particles with radius a, this force density and the stress can be written as

$$\theta_{\mathrm{d}} \boldsymbol{F}_{\mathrm{d}}(\boldsymbol{x}, t) = n(\boldsymbol{x}, t) \int_{|\boldsymbol{r}|=a} [\langle \boldsymbol{\sigma}_{\mathrm{c}} \rangle_1 (\boldsymbol{x} + \boldsymbol{r}, t | \boldsymbol{x}) - \langle \boldsymbol{\sigma}_{\mathrm{c}} \rangle (\boldsymbol{x} + \boldsymbol{r}, t)] \cdot \boldsymbol{n} \mathrm{d}S_r, \tag{50}$$

$$\theta_{\mathrm{d}} \boldsymbol{T}(\boldsymbol{x}, t) = a\ n(\boldsymbol{x}, t) \int_{|\boldsymbol{r}|=a} [\langle \boldsymbol{\sigma}_{\mathrm{c}} \rangle_1 (\boldsymbol{x} + \boldsymbol{r}, t | \boldsymbol{x}) - \langle \boldsymbol{\sigma}_{\mathrm{c}} \rangle (\boldsymbol{x} + \boldsymbol{r}, t)] \cdot \boldsymbol{n}\boldsymbol{n} \mathrm{d}S_r, \tag{51}$$

where $n(\boldsymbol{x}, t)$ is the number density of the particles, and $\langle \boldsymbol{\sigma}_{\mathrm{c}} \rangle_1$ is the average stress on the particle surface under the condition that the particle center is located at $\boldsymbol{x}$.

The force $\boldsymbol{F}_{\mathrm{d}}$ includes the drag, added mass force, the Basset force, etc. The stress $\boldsymbol{T}$ represents the dynamic part of the stress difference between the disperse and the continuous phases. In the case of a potential flow, the trace of this stress is related to the difference between the pressure averaged over particle surfaces and the average pressure of the continuous phase (Stuhmiller, 1977; Zhang and Prosperetti, 1994). This pressure difference is caused by the Bernoulli effect. With (49), the momentum equation for the continuous phase becomes

$$\frac{\partial}{\partial t}(\theta_{\mathrm{c}} \langle \rho_{\mathrm{c}}^0 \rangle \tilde{\boldsymbol{u}}_{\mathrm{c}}) + \nabla \cdot (\theta_i \langle \rho_{\mathrm{c}}^0 \rangle \tilde{\boldsymbol{u}}_{\mathrm{c}} \tilde{\boldsymbol{u}}_{\mathrm{c}}) = \theta_{\mathrm{c}} \nabla \cdot \langle \boldsymbol{\sigma}_{\mathrm{c}} \rangle + \nabla \cdot (\theta_{\mathrm{c}} \boldsymbol{\sigma}_{\mathrm{c}}^{Re}) + \nabla \cdot (\theta_{\mathrm{d}} \boldsymbol{T}) - \theta_{\mathrm{d}} \boldsymbol{F}_{\mathrm{d}} + \int \dot{C}_{\mathrm{c}} \rho_{\mathrm{c}}^0 \boldsymbol{u}_{\mathrm{c}} \mathrm{d}\mathscr{P}. \tag{52}$$

The interfacial force $\boldsymbol{f}_{\mathrm{d}}$ in the momentum equation for the disperse phase can be related to $\boldsymbol{f}_{\mathrm{c}}$ using (16). Upon the application of the small particle approximation, the surface tension effect represented by the right hand side of (16) can be written as divergence of a stress (Prosperetti and Zhang, 1996), because the integral of the surface tension force over a particle surface yields zero net force (Hesla et al., 1993; Prosperetti and Jones, 1984). This stress tensor due to the surface tension together with the dynamical stress difference $\boldsymbol{T}$ from $\boldsymbol{f}_{\mathrm{c}}$ cancels the corresponding part of the stress difference $\langle \boldsymbol{\sigma}_{\mathrm{d}} \rangle - \langle \boldsymbol{\sigma}_{\mathrm{c}} \rangle$ in the momentum Eq. (15) for the disperse phase $(i = d)$ (Prosperetti and Zhang, 1996). Using Eqs. (33), (47), (53) and (54) in that paper one finds that, in the momentum equation for the disperse phase, the only part of the stress difference left is the stress due to particle collisions besides a term negligible under the small particle approximation. Hence the momentum equation for the disperse phase can be written as

$$\frac{\partial}{\partial t}(\theta_{\mathrm{d}} \langle \rho_{\mathrm{d}}^0 \rangle \tilde{\boldsymbol{u}}_{\mathrm{d}}) + \nabla \cdot (\theta_{\mathrm{d}} \langle \rho_{\mathrm{d}}^0 \rangle \tilde{\boldsymbol{u}}_{\mathrm{d}} \tilde{\boldsymbol{u}}_{\mathrm{d}}) = \theta_{\mathrm{d}} \nabla \cdot \langle \boldsymbol{\sigma}_c \rangle + \nabla \cdot (\theta_{\mathrm{d}} \boldsymbol{\sigma}_{\mathrm{d}}^{Re}) + \nabla \cdot (\theta_{\mathrm{d}} \boldsymbol{\sigma}_{\mathrm{coll}}) + \theta_{\mathrm{d}} \boldsymbol{F}_{\mathrm{d}} + \int \dot{C}_{\mathrm{d}} \rho_{\mathrm{d}}^0 \boldsymbol{u}_{\mathrm{d}} \mathrm{d}\mathscr{P}, \tag{53}$$

where $\boldsymbol{\sigma}_{\mathrm{coll}}$ is the stress due to particle collisions (Zhang and Rauenzahn, 1997, 2000).

References

Ash, R.B., 1972. Real Analysis and Probability. Academic Press, Inc., Orlando, FL.

Bentsen, R.G., 2003. The role of capillarity in two-phase flow through porous media. Transport Porous Med. 51, 103–112.

Cummins, S.J., Brackbill, J.U., 2002. An implicit particle-in-cell method for granular materials. J. Comput. Phys. 180, 506–548.

Drew, D.A., Passman, S.L., 1999. Ensemble averaging. Theory of Multicomponent fluids. Springer-Verlag, New York, NY (Chapter 9).

Feng, X.-Q., Mai, Y.-W., Qin, Q.-H., 2003. A micromechanical model for interpenetrating multiphase composites. Comp. Mater. Sci. 28, 486–493.

Glimm, J., Saltz, D., Sharp, D.H., 1999. Two-phase modeling of a fluid mixing layer. J. Fluid Mech. 378, 119–143.

Harlow, F.H., Amsden, A.A., 1991, Fluid dynamics, A LASL Monograph, Los Alamos National Laboratory Report LA-4700.

Hesla, T.I., Huang, A.Y., Joseph, D.D., 1993. A note on the net force and moment on a drop due to surface forces. J. Coll. Interface Sci. 158, 255–257.

Hwang, G.J., Shen, H.H., 1989. Modeling the solid phase stress in a fluid–solid mixture. Int. J. Multiphase Flow 15.

Kashiwa, B.A., Rauenzahn, R.M., 1994. A multimaterial formalism. In: Crowe, C.C., Johnson, R., Prosperetti, A., Sommerfeld, M., Tsuji, Y. (Eds.), Numerical Method in Multiphase flows, FED-Vol 185. ASME, New York.

Ma, X., Zou, Q., Zhang, D.Z., VanderHeyden, W.B., Wathugala, G.W., Hasselman, T.K., 2005. Application of a FILP-MPM-MFM method for simulating weapon-target interaction. In: Proceedings of the 12th International Symposium on Interaction of the Effects of Munitions with Structures, New Orleans, Louisiana, September 13–16.

Pan, Y., Dudukovic, M.P., Chang, M., 2000. Numerical investigation of gas-driven flow in 2-D bubble columns. AIChE J. 46, 434–449.

Prosperetti, A., 1999. Some considerations on the modeling of disperse multiphase flows by averaged equations. JSME Int. J. Series B 42, 573–585.

Prosperetti, A., Jones, A.V., 1984. Pressure forces in disperse two-phase flows. Int. J. Multiphase Flow 10, 425–440.

Prosperetti, A., Tryggvason, G., 2006. Computational Methods for Multiphase Flow. Cambridge University Press (Chapter 10).

Prosperetti, A., Zhang, D.Z., 1996. Disperse phase stress in two-phase flow. Chem. Eng. Comm. 141-142, 387–398.

Ramshaw, J.D., 1998. Simple model for linear and nonlinear mixing at unstable fluid interfaces with variable acceleration. Phys. Rev. E 58, 5834–5840.

Saltz, D., Lee, W., Hsiang, T.-R., 2000. Two-phase flow analysis of unstable fluid mixing in one-dimensional geometry. Phys. Fluid. 12, 2461–2477.

Sangani, A.S., Didwania, A.K., 1993. disperse-phase stress tensor in flows of bubbly liquids at large Reynolds numbers. J. Fluid Mech. 248, 27–54.

Stuhmiller, J.H., 1977. The influence of interfacial pressure forces on the character of the two-phase flow model equations. Int. J. Multiphase Flow 3, 551–560.

Sulsky, D., Brackbill, J.U., 1991. a numerical method of suspension flow. J. Comput. Phys. 96, 339–368.

Sundaresan, S., 2000. Modeling the hydrodynamics of multiphase flow reactors: Current status and challenges. AIChE J. 46, 1102–1105.

Wegner, L.D., Gibson, L.J., 2000. The mechanical behaviour of interpenetrating phase composites - I: modeling. Int. J. Mech. Sci. 42, 925–942.

Yosida, K., 1966. Functional Analysis. Springer-Verlag, New York.

Zhang, D.Z., Prosperetti, A., 1994. Averaged equations fro inviscid disperse two-phase flow. J. Fluid Mech. 267, 185–219.

Zhang, D.Z., Prosperetti, A., 1997. Momentum and energy equations for disperse two-phase flow and their closure for dilute suspensions. Int. J. Multiphase Flow 23, 425–453.

Zhang, D.Z., Rauenzahn, R.M., 1997. A viscoelastic model for dense granular flow. J. Rheol. 41, 1275–1298.

Zhang, D.Z., Rauenzahn, R.M., 2000. Stress relaxation in dense and slow granular flows. J. Rheol. 45, 1019–1023.

Zhang, D.Z., VanderHeyden, W.B., 2001. High-resolution three-dimensional numerical simulation of a circulating fluidized bed. Powder Tech. 116, 133–141.

Zhang, D.Z., VanderHeyden, W.B., 2002. The effects of mesoscale structures on the macroscopic momentum equations for two-phase flows. Int. J. Multiphase Flow 28, 805–822.